

# Two-photon induced photorefraction in undoped lithium tantalate crystals with different compositions

I.S. Steinberg · I.E. Kalabin · P.E. Tverdokhle

Received: 30 November 2008 / Revised version: 19 January 2009 / Published online: 28 February 2009  
© Springer-Verlag 2009

**Abstract** Two-photon interband photorefraction in undoped lithium tantalate crystals with composition ranging from 47.95 to 49.6 mol% of lithium oxide was demonstrated at the wavelength of 532 nm. The photorefractive properties were examined with holographic method. Two-photon holograms were recorded with high holographic sensitivity, large refractive index change, and fast hologram writing time. Permanent changes of the refractive index have been obtained. These holograms can be read nondestructively at the wavelength of 660 nm using heterodyne method. Holographic characteristics strongly depend on composition.

**PACS** 42.40.Ht · 42.50.Hz · 42.70.Ln · 42.70.Jk

## 1 Introduction

Conventional photorefraction in ferroelectric crystals doped with transition metal impurities has been investigated in detail [1]. This effect is based on photoionization of impurities and subsequent charge transport. The absorption of the material is small and it leads to a slow photoexcitation process. As discussed in [2], a faster photoexcitation can be obtained by using a wavelength that is more efficient in producing free charges, i.e., with photon energies above the

band edge. In this case the intrinsic density of potentially available charges is substantially higher than the density of midgap impurities levels and therefore, it is possible to ignore dopants. However, the strong linear absorption impedes the homogeneity on depth recording. This problem can be solved by the use of two-photon interband photoexcitation. The latter can be achieved in the case of two-photon absorption (TPA) in focused light beams when light-induced modification takes place only near the focal point where the light intensity is maximal. This feature of TPA allows to spatially localize the area of photoinduced modification. The other advantage of TPA implementation is a possibility of nondestructive reading. Therefore, the method of two-photon interband photoexcitation provides an ideal tool for studying of the intrinsic photorefractive effect in undoped ferroelectric crystals.

The experiments aimed at two-photon recording have been carried out earlier in congruent pure and doped lithium niobate ( $\text{LiNbO}_3$ ) [3] and lithium tantalate ( $\text{LiTaO}_3$ ) [4] crystals. However, only congruent samples were investigated.

This paper addresses the photorefractive properties of undoped  $\text{LiTaO}_3$  at two-photon excitation as the function of the crystal composition. We have selected several crystals with different  $\text{Li}/(\text{Li} + \text{Ta})$  ratio in the bulk. The birefringence of the crystals was determined. The photorefractive properties were measured with our holographic experimental setup.

## 2 Samples

The  $\text{LiTaO}_3$  crystals with a diameter of 10–16 mm were grown by Czochralski method from initial charges with different compositions  $x = \text{Li}/(\text{Li} + \text{Ta})$ . Monodomenization of the boules was produced by slow cooling through the

I.S. Steinberg (✉) · P.E. Tverdokhle  
Institute of Automation and Electrometry, Siberian Branch  
of the Russian Academy of Sciences, Novosibirsk 630090, Russia  
e-mail: [steinberg@iae.nsk.su](mailto:steinberg@iae.nsk.su)  
Fax: +7-383-3333863

I.E. Kalabin  
Institute of Semiconductor Physics, Siberian Branch  
of the Russian Academy of Sciences, Novosibirsk 630090, Russia

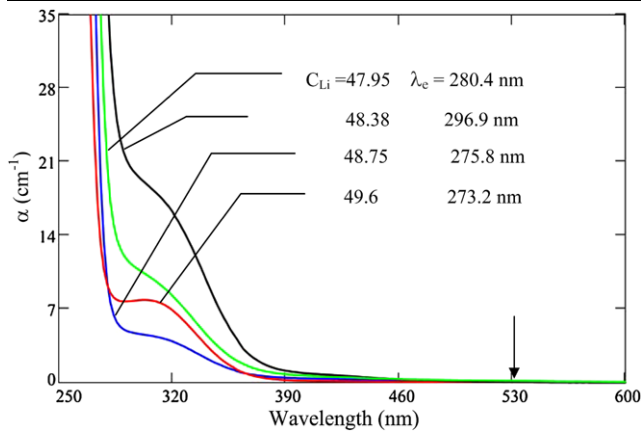


**Fig. 1** Absorption spectra of LiTaO<sub>3</sub> crystals with different compositions  $x = \text{Li}/(\text{Li} + \text{Ta})$ . The recording wavelength ( $\lambda = 532 \text{ nm}$ ) is indicated by the arrow

**Table 1** Lithium molar concentration, obtained from the values of the birefringence, according to [5–7] and [8]

$\delta n = n_e - n_o$	0.0077	0.0046	0.0038	−0.0007
$C_{\text{Li}}$ (mol%) according [5–7]	47.95	48.38	48.75	49.6
$C_{\text{Li}}$ (mol%) according to [8]	47.84	48.76	48.92	49.63

Curie point in electrical field applied to (001) crystal faces. Then, single crystals were cut into parallelepipeds. All edges were directed along basic crystallographic axes. The real value of  $x$  for every sample was identified through the reference to the value of the birefringence  $\Delta n = n_e - n_o$  using previously defined calibration curve [5]. The birefringence is measured by the prism coupling method with wavelength of 633 nm. The uncertainty is about  $\pm 0.0002$  [6]. This way provides the Li/(Ta + Li) molar ratio determination with a possible error of  $\pm 0.001$ . It is defined mainly by an accuracy of the Curie temperature  $T_C$  dependence on the Li/(Li + Ta) ratio. The calibration curve  $T_C(x)$  reported in [7] is used in our calculations.

Four LiTaO<sub>3</sub> samples with lithium molar concentrations of 47.95, 48.38, 48.75, and 49.6 were selected (Table 1). For the same values of birefringence, in Table 1 we give the data of the Li molar concentration of the crystals obtained in [8]. Table 1 shows that the results for low and high lithium content are close, but for intermediate compositions the difference is more significant.

Congruently melting LiTaO<sub>3</sub> has lithium concentration of about 48.5 mol%. Therefore, the samples under research range from so-called under-congruent crystal (47.95 mol%) to nearly stoichiometric one (49.6 mol%).

Figure 1 shows the absorption spectra of LiTaO<sub>3</sub> crystals. They were measured with a Shimadzu UV-3100 spectrophotometer. The values of the absorption edge  $\lambda_e$  determined at the level  $\alpha = 20 \text{ cm}^{-1}$  are also indicated. The increase

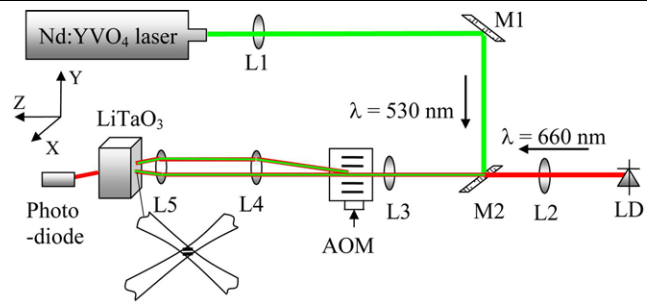


**Fig. 2** Optical scheme of the experimental setup for two-photon recording and heterodyne reading of the microholograms

**Table 2** Concentration of iron determined by absorption spectra according to [9]

$C_{\text{Li}}$ (mol%)	47.95	48.38	48.75	49.6
$C_{\text{Fe}^{2+}} (\times 10^{17} \text{ cm}^{-3})$	1.43	1.96	2.13	0.36
$C_{\text{Fe}^{3+}} (\times 10^{17} \text{ cm}^{-3})$	5.12	9.65	2.35	4.16
$C_{\text{Fe}} (\times 10^{17} \text{ cm}^{-3})$	6.55	11.61	4.48	4.52

of lithium concentration leads to UV shift of the absorption edge to shorter wavelength and, hence, to the increase of the band-gap energy. Only the sample with  $C_{\text{Li}} = 48.38 \text{ mol}\%$  falls out from this well-known regularity.

According to [9] the absorption coefficients for ordinarily polarized light at 400 and 310 nm yield the concentration  $C_{\text{Fe}^{2+}}$  and  $C_{\text{Fe}^{3+}}$ . Table 2 lists the iron concentration obtained by this method. If we assume that the most common uncontrollable impurity is iron, these samples can be considered conventionally undoped because, as we see from Table 2, its concentration  $C_{\text{Fe}}$  is less than  $10^{18} \text{ cm}^{-3}$  in all samples.

### 3 Experimental methods

Two-photon recording of the volume holograms in LiTaO<sub>3</sub> and their subsequent collinear heterodyne detection with the amplitude and the phase reconstruction was carried out on the experimental setup. The optical scheme of this setup is illustrated in Fig. 2. A second harmonic radiation from compact diode pump Q-switched solid-state laser on the basis neodymium: yttrium orthovanadate (Nd:YVO<sub>4</sub>) ( $\lambda = 530 \text{ nm}$ , pulse duration of  $\tau_p = 1.7 \text{ ns}$ ) is used for recording of the volume holograms. The maximum repetition rate is 10 kHz. The optical system consisting of lenses L1, L3 and mirrors M1, M2 forms a waist in the acousto-optic modulator (AOM). The light beam received as a result of diffraction and the zero beam with the help of the telescopic system L4, L5 are matched in the volume of the LiTaO<sub>3</sub> crystal where the hologram is recorded. Measurements have shown that

the size of the hologram is  $X \times Y = 1.0 \times 1.4 \mu\text{m}^2$ , the spatial frequency is  $1030 \text{ mm}^{-1}$ . Since these holograms consist of only two or three fringes, we call them microholograms. The numerical aperture of the microscope objective L5 is 0.65. The maximum energy of the green laser pulse on the sample surface is  $2.2 \times 10^{-7} \text{ J}$  and peak light intensity is  $I = 5.8 \text{ GW/cm}^2$ .

Heterodyne reading is carried out with the help of the semiconductor laser at wavelength of 660 nm and light power of 8 mW. The laser radiation is collimated by lens L2, and then passes through the same optical system, as the recording beams, and forms a micrograting (optical interference pattern) in the same place and with the same spatial frequency. The micrograting size is  $X \times Y = 1 \times 1.5 \mu\text{m}^2$ . A more detailed description of the method of heterodyne reading has been given in our previous papers [10].

The  $C$  axis of the crystals is placed parallel both to the surface of the sample and the plane of incidence of the interfering beams. The recording ( $\lambda = 530 \text{ nm}$ ) and reading ( $\lambda = 660 \text{ nm}$ ) beams have extraordinary polarization.

Since the recording is related to light beam absorption, it is important to estimate the proportion of the linear and nonlinear parts of the absorption coefficient in the undoped  $\text{LiTaO}_3$ . Considering that the energy of two photons  $2\hbar\omega = 4.68 \text{ eV}$  exceeds the energy gap  $E_g \sim (4.1\text{--}4.36) \text{ eV}$  of  $\text{LiTaO}_3$  samples, TPA occurs in it. The optical band gap was estimated by absorption spectra according to the equation  $\alpha(\omega) \propto (\hbar\omega - E_g)^2/\omega$  that described the absorption edge of amorphous semiconductors and dielectrics [11]. The value of the TPA coefficient for pure  $\text{LiTaO}_3$  is  $\beta = 2 \times 10^{-9} \text{ cm/W}$  at  $\lambda = 400 \text{ nm}$  and is evaluated in [12]. The dependence of the TPA coefficient on the energy of absorbed photons in a two-band model can be written in the form  $\beta \sim (2\hbar\omega - E_g)^{3/2}$  [13], and at  $\lambda = 530 \text{ nm}$  the estimation gives  $\beta \approx (0.12\text{--}0.24) \text{ cm/GW}$  for the crystals under research. The nonlinear part of the absorption coefficient is defined as  $\alpha_2 = \beta I$ , where  $I$  denotes writing light intensity. The value of this part for  $I = 5 \text{ GW/cm}^2$  is equal  $\alpha_2 = (0.6\text{--}1.2) \text{ cm}^{-1}$ . The value of a linear absorption coefficient on the same wavelength is  $\alpha_1 < 0.05 \text{ cm}^{-1}$  (see Fig. 1). Therefore, the linear part of the absorption can be ignored and TPA is the determining factor of recording.

The recording process is carried out as follows: two sharp focused laser beams overlap in the volume of the crystal. Simultaneous absorption of two photons implies interband photoexcitation of electrons. We suggest that further there operates traditional mechanism of the permanent hologram formation, i.e., electrons redistribution and their trapping in empty centers. We do not understand the nature of these centers yet. A space charge field builds up the refractive index changes and a volume microhologram is formed. The indirect verification of this suggestion can be seen in the results of the interband photorefractive induced by the linear absorption of the UV radiation [2, 14].

Comparison of the efficiency of the microholograms reading for ordinarily and extraordinarily polarized beams was carried out. It is well known that the contrast of grating formed by ordinarily polarized beams is higher, but at the incidence angle of  $19^\circ$  (in the air) the difference in contrast is only 2%. However, because the electro-optic coefficient  $r_{33}$  for extraordinarily polarized light is about three times more than the coefficient  $r_{13}$  for ordinarily polarized light, the efficiency of microholograms reading by the extraordinarily polarized beams must be also about three times more. The carried out experiment has validated that the ratio of the refractive index change for extraordinarily and ordinarily polarized reading beams  $\Delta n_e/\Delta n_o$  is in a range of 2.5–3. Such an experiment provides an additional argument that after two-photon excitation a hologram is forming through a traditional photorefractive mechanism.

Recording was carried out for several values of the light intensity. For each value of the intensity recording of several lines of four microholograms located in the volume of  $\text{LiTaO}_3$  is performed.

#### 4 Experimental results

Figure 3 shows the refractive index change as a function of the writing beam intensity for three samples with different lithium concentration. The light intensity was varied with neutral density filters. The curves in Fig. 3 are the fits according to  $\Delta n = aI + bI^2$ , where  $a$  and  $b$  represent the free parameters, and  $I$ —the writing light intensity. The quadratic in intensity term testifies to the two-photon absorption mechanism at microhologram formation. At the high light intensity of  $\sim 5 \text{ GW/cm}^2$  the contribution of this term is  $\sim 60\text{--}90\%$ .

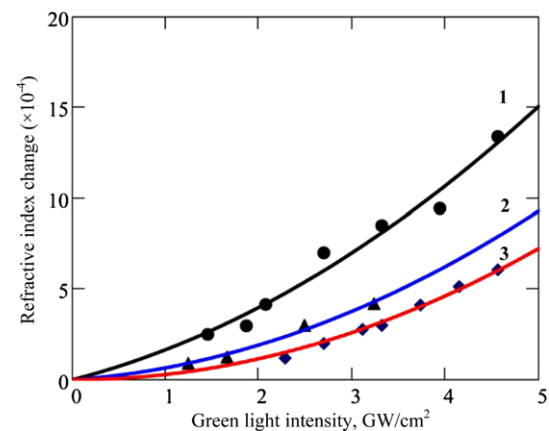


**Fig. 3** Dependence of two-photon-induced refractive index change vs total writing intensity for exposure by a train of eight pulses in crystals with different lithium concentration  $C_{\text{Li}}$ : 1–48.38 mol%; 2–48.75 mol%; 3–49.6 mol%

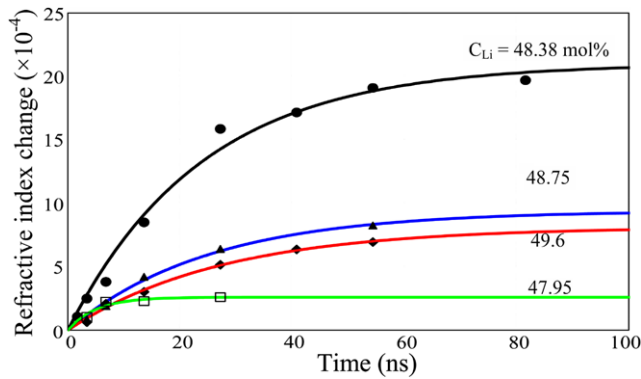


**Fig. 4** Time dynamics of refractive index change during recording in crystals with different compositions. The light intensity is  $I = 3.3 \text{ GW/cm}^2$

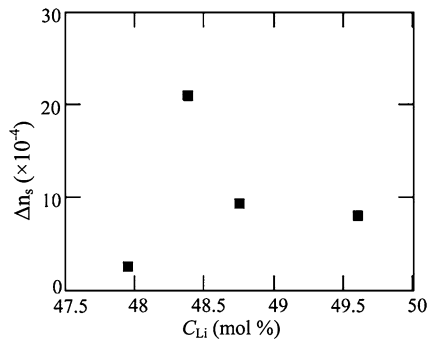


**Fig. 5** Saturation value of refractive index change ( $\lambda = 660 \text{ nm}$ ) vs lithium concentration. The reading light intensity is  $I = 10^5 \text{ W/cm}^2$

In [15] it is shown that in conventionally pure  $\text{LiTaO}_3$  ( $C_{\text{Fe}} \sim 10^{18} \text{ cm}^{-3}$ ) at a light intensity  $\sim 1 \text{ W/cm}^2$  the saturation value of the refractive index change is  $\Delta n_s \sim 10^{-5}$ . This value is well matched to the residual concentration of iron. Considerably bigger values of the refractive index change, received at a light intensity of  $\sim 5 \text{ GW/cm}^2$ , show that here a different recording mechanism takes place.

The time dynamics of the microholograms was also studied. Figure 4 shows the temporal development of the refractive index change during recording in crystals with different lithium concentration. The timescale corresponds to the exposure time of the green light, i.e., after  $k$  pulses we obtain the exposure time  $t = k\tau_p$  and the intervals between impulses were not taken into account. All the curves are well described by monoexponential function

$$\Delta n = \Delta n_s (1 - \exp(-t/\tau)), \quad (1)$$

where  $\Delta n_s$  is the saturation value of refractive index change,  $\tau$  is the recording time constant, and  $t$  is the exposure time. The recording time constant and saturation value of refractive index change (see Fig. 5) depend on lithium concentration.

Figure 5 shows the dependence of the saturation value of refractive index change on the lithium concentration deter-

mined from the data on the Fig. 4. The minimum value of the recording time constant  $\tau = 24 \text{ ns}$  and the greatest saturation value of refractive index change  $\Delta n_s = 21 \times 10^{-4}$  are reached at the lithium concentration of 48.38 mol%. All measurements were done at light intensity  $I = 3.3 \text{ GW/cm}^2$ . While in the two-color recording in iron-doped congruent  $\text{LiTaO}_3$ , the obtained values with continuous-wave (cw) laser were  $\tau \sim 2 \text{ s}$  and  $\Delta n_s = 1 \times 10^{-5}$  [16], and with high-intensity laser pulses the results were  $\tau = 500 \text{ ns}$  and  $\Delta n_s = 1.6 \times 10^{-4}$  [9]. One can see that two-photon interband photoexcitation of electrons leads to much faster photorefractive response time  $\tau$  in contrast to the conventional case where charges get photoexcited from midgap impurity centers. A similar relation is observed at interband phototransitions in  $\text{LiTaO}_3$  at linear absorption of UV radiation [14]. The response time for such transitions is three orders of magnitude faster than the response time related to phototransitions from midgap defect levels.

We can calculate a holographic recording sensitivity  $S$  from the data in Fig. 4. It is defined as

$$S = \frac{1}{Id} \left. \frac{\partial \sqrt{\eta}}{\partial t} \right|_{t=0}, \quad (2)$$

where  $I$  is the total writing intensity and  $d$  is the size of the hologram on depth. For  $d = 10 \mu\text{m}$ ,  $I = 3.32 \text{ GW/cm}^2$ , and for the upper curve in Fig. 4 one obtains  $S = 1.3 \text{ cm/J}$ .

We have obtained the best results in the sample with  $C_{\text{Li}} = 48.38 \text{ mol\%}$ , but we are not sure here we deal only with dependence related to the composition changes because this crystal has some additional absorption in the near UV region and a smaller value of the optical band gap. As stated above, the coefficient of TPA strongly depends on the difference between energies of two quanta and energy gap. In our case the energy of two quanta  $2\hbar\omega = 4.68 \text{ eV}$  only slightly exceeds the energy gap of the samples, and small energy gap changes can imply considerable changes of the TPA coefficient. The estimation of the TPA coefficient carried out according to the theoretical model [13] gives for the crystal with energy gap  $E_g \approx 4.1 \text{ eV}$  the value of the TPA coefficient in about two times more than for the sample with  $C_{\text{Li}} = 48.75\%$  ( $E_g \approx 4.3 \text{ eV}$ ). It is the presence of impurity in such concentration ( $\sim 10^{18} \text{ cm}^{-3}$ ) that seems to produce the long-wave shift of the absorption edge and thus to influence the value of the TPA coefficient. In other samples the impurity concentration is about two to three times less and a UV shift regularity of the absorption spectrum at Li concentration increasing is not broken. We consider that in these samples the dependence of the composition changes might be the crucial factor in the formation of the saturation value of the refractive index change.

The experiments on heterodyne reading in all  $\text{LiTaO}_3$  crystals under research have shown that nonvolatile reading

is possible at a wavelength of 660 nm. After the initial decrease by 15–20%, the value of the refractive index change virtually stabilizes and remains constant, within at least 1 h of continuous reading. It should be mentioned that the reading intensity is rather high ( $10^5$  W/cm<sup>2</sup>). Therefore, we can conclude that under two-photon interband photoexcitation we obtained permanent changes of the refractive index.

## 5 Conclusion

We have demonstrated the two-photon interband holographic recording and nonvolatile reading in undoped LiTaO<sub>3</sub> with different composition. Even though the underlying photorefraction mechanisms in undoped LiTaO<sub>3</sub> remain unclear, the experimental results show that the two-photon recording provides high values of refractive index change  $\Delta n = 21 \times 10^{-4}$ , holographic recording sensitivity  $S = 1.3$  cm/J, and recording time constant  $\tau = 24$  ns. Holographic characteristics strongly depend on the Li/(Li + Ta) ratio. The size of the transmitting microhologram is  $1.0 \times 1.4 \times 10$   $\mu\text{m}^3$ . Since we used small-sized holograms we could increase the light intensity in a region of recording up to 5 GW/cm<sup>2</sup> by using a very compact laser source.

**Acknowledgements** This research was supported by the programme for interdisciplinary cooperation of the Siberian Branch of the Russian Academy of Sciences (grant No 71). The authors appreciate the contributions by Yu. A. Shepetkin, V.V. Atuchin, and N.N. Vyukhina to this study.

## References

1. K. Buse, J. Imbrock, E. Krätzig, K. Peithmann, in *Photorefractive Materials and Their Applications 2*, ed. by P. Günter, J.-P. Huignard (Springer, Berlin, 2007), p. 83. Chap. 4
2. G. Montemezzani, P. Rogin, M. Zgonik, P. Günter, *Phys. Rev. B* **49**, 2484 (1994)
3. D. von der Linde, A.M. Glass, K.F. Rodgers, *Appl. Phys. Lett.* **25**, 155 (1974)
4. I.S. Steinberg, Y.A. Shepetkin, *Appl. Opt.* **47**, 9 (2008)
5. V.V. Atuchin, *Opt. Spectrosc.* **67**, 771 (1989)
6. H. Onodera, I. Awai, J. Ikenoue, *Appl. Opt.* **22**, 1194 (1983)
7. R.L. Barns, J.R. Carruthers, *J. Appl. Crystallogr.* **3**, 395 (1970)
8. J. Imbrock, C. Bäumer, F. Holtmann, H. Hesse, E. Krätzig, D. Kip, in *Photorefractive Effects, Materials and Devices*. OSA TOPS, vol. 87 (2003), p. 15
9. J. Imbrock, S. Wevering, K. Buse, E. Krätzig, *J. Opt. Soc. Am. B* **16**, 1392 (1999)
10. A.Y. Belikov, N.N. V'yukhina, V.N. Zatulokin, P.E. Tverdokhlebl, A.V. Trubetskoi, I.S. Steinberg, Y.A. Shchepetkin, *Optoelectron. Instrum. Data Process.* **43**, 59 (2007)
11. J. Tauc, R. Grigorovici, A. Vancu, *Phys. Status Solidi* **15**, 627 (1966)
12. A. Carson, M. Anderson, *J. Opt. Soc. Am. B* **23**, 1129 (2006)
13. V.I. Bredikhin, M.D. Galanin, V.N. Genkin, *Phys. Uspekhi* **16**, 299 (1973)
14. P. Dittrich, B. Koziarska-Glinka, G. Montemezzani, P. Günter, *J. Opt. Soc. Am. B* **21**, 632 (2004)
15. J. Imbrock, C. Bäumer, H. Hesse, D. Kip, E. Krätzig, *Appl. Phys. B* **78**, 615 (2004)
16. J. Imbrock, D. Kip, E. Krätzig, *Opt. Lett.* **24**, 1302 (1999)